Temperature and bias anomalies in the photoluminescence of InAs quantum dots coupled to a Fermi reservoir

A. R. Korsch,[1,*] G. N. Nguyen,[1] M. Schmidt,[1] C. Ebler,[1] S. R. Valentin,[1] P. Lochner,[1,2] C. Rothfuchs,[1] A. D. Wieck,[1] and A. Ludwig[1]

[1]*Lehrstuhl für Angewandte Festkörperphysik, Ruhr-Universität Bochum, Universitätsstraße 150, D-44780 Bochum, Germany*

[2]*Fakultät für Physik and CENIDE, Universität Duisburg-Essen, Lotharstraße 1, D-47048 Duisburg, Germany*

(Received 25 February 2019; revised manuscript received 21 March 2019; published 4 April 2019)

We present anomalous behavior of temperature-dependent photoluminescence (PL) measurements on InAs quantum dot ensembles coupled to an electron reservoir in an *n-i-p* diode structure. When negative gate voltages are applied to the sample, an anomalous initial increase of the integrated PL signal with rising temperature is observed for the ground-state and first-excited-state emission peaks. In contrast, measurements at positive gate voltages show no such anomaly and are well described by the commonly used Arrhenius model. Unlike previous studies on uncoupled quantum dot ensembles, we show that in quantum dot diode structures the anomalous temperature dependence and its dependence on the applied bias voltage is dominated by electrons tunneling from the electron reservoir to the quantum dots. Tunneling electrons enhance the PL signal by recombining with holes stored in the quantum dots and the tunneling rate depends on temperature via the Fermi distribution in the electron reservoir. With the implementation of a rate-based tunnel coupling, we develop a modified Arrhenius model that takes the observed anomalies excellently into account. Gate voltage dependent PL measurements at 77 K are further compared to capacitance-voltage spectroscopy measurements on the same sample, supporting the proposed interpretation. The PL peak width shows a characteristic evolution as a function of temperature, which is discussed qualitatively in terms of our model.

DOI: 10.1103/PhysRevB.99.165303

I. INTRODUCTION

Self-assembled InAs quantum dots (QDs) in semiconductor heterostructures provide a model system for the study of three-dimensional carrier confinement. Their discrete energy level structure and exceptional optical properties enabled the realization of new technologies such as QD lasers [1–4] or single-photon sources [5–7]. For many applications, QDs are embedded in diode structures, in which an applied gate voltage is used to tune the energy levels and charge QDs with small discrete numbers of electrons or holes [8,9]. For this reason, a thorough characterization of physical phenomena occurring in such structures is indispensable for advancing their technological applicability and has hence been an active area of research for many years.

In QD diode structures, the coupling of QDs to an electron reservoir at varying gate voltages leads to a variety of different effects: The appearance of various exciton species (negatively charged at positive bias up to X^{6-}; positively charged at negative bias up to X^{6+}) in optical spectroscopy of single QDs has been reported by, e.g., Ediger *et al.* [8]. They found that the more carriers that are present the more diverse are the initial and final states for carrier recombinations leading to a multiplet of lines in the spectra. Recombination rates of excitonic states are determined by the respective minority charge carriers, i.e., holes in negatively charged excitons and electrons in positively charged excitons. Recently, positively charged excitonic states up to X^{5+} have also been investigated electronically in capacitance-voltage spectroscopy of QD ensembles [10]. Moreover, excitonic states with more than two carriers give rise to Auger effects [11]. The availability of electrons in the back contact further leads to spatially indirect recombinations of these electrons with holes stored in the QDs [12]. Furthermore, free electrons generated by photoexcitation from the electron reservoir can be captured by QDs [13].

Of particular concern for the realization of optoelectronic devices in general and specifically QD devices is the operation at ambient conditions and the temperature dependence of optical emission properties, which has been studied extensively [14–18]. Temperature-dependent photoluminescence (PL) measurements are a common method for determining activation energies of carrier escape mechanisms from the QDs or nonradiative recombination centers providing states in the band gap, at which the Shockley-Read-Hall recombination can occur [19,20]. Both of these processes are thermally activated. The temperature-dependent behavior of the integrated PL signal is usually described by a simple model, in which thermal activation of nonradiative recombination or escape channels is treated by an Arrhenius model [21,22]. The integrated PL signal I as a function of temperature T is described by

$$I = \frac{I_0}{1 + \sum_i c_i \exp\left(-\frac{E_{\mathrm{a},i}}{k_\mathrm{B} T}\right)}, \tag{1}$$

where the sum is taken over all possible nonradiative recombination or escape channels and I_0, the activation rates

*Corresponding author: alexander.korsch@rub.de

c_i and the activation energies $E_{a,i}$ of each channel are fit parameters. I_0 corresponds to the integrated PL signal when the temperature approaches 0 K. A monotonic decrease of the integrated PL signal with rising temperature is the result.

One might suspect that temperature-dependent PL measurements on a QD diode structure, to which a gate voltage is applied, could be used to selectively characterize nonradiative recombination channels related to holes or electrons by determining their activation energies from a fit using the Arrhenius model (1): Since at positive gate voltages holes are minority charge carriers in the QDs, the temperature dependence of the PL signal is expected to mainly depend on defect states related to holes and vice versa for electron-related defect states at negative gate voltages. However, in our present work we demonstrate that, in QD diode structures, in which QDs are separated from an electron reservoir by a tunneling barrier, this tunnel coupling leads to anomalous temperature dependence of the PL signal. These effects significantly impede the feasibility of electron-hole resolved defect state characterization.

In particular, we investigate the behavior of the PL signal for QD diode structures at varying temperatures and gate voltages. Unlike previous studies on uncoupled quantum dot ensembles, which report an anomalous temperature dependence of the PL signal [17,18,23,24], we show that in QD diode structures the temperature dependence of the PL signal is strongly affected by the applied gate voltage: We demonstrate that the approximation of the Arrhenius model is valid only for the ground state emission for a range of weakly negative and positive gate voltages. An anomalous increase of integrated PL signal and a minimum in the full width at half maximum (FWHM) as a function of temperature are found at negative gate voltages. While we also discuss explanations reported in previous studies [18,23], both observations are mainly attributed to thermally activated tunnel coupling to an electron reservoir in the structure: Electrons from the back contact can tunnel into the QDs and recombine with stored holes enhancing the PL signal. This process depends on temperature through the electron Fermi distribution in the back contact. A modified Arrhenius model for fits of the ground-state integrated PL signal is proposed to take this effect into account. Excited-state emission peaks in the spectra show even stronger anomalous temperature dependence as they are additionally influenced by thermal redistribution to higher energy levels within the QDs as well as state filling effects.

The paper is structured as follows: In Sec. II, we discuss the sample design and properties as well as the experiments. The results are presented in Sec. III starting from the measurements of integrated PL signal of the individual peaks in the spectra at varying temperatures and gate voltages. We further compare the PL signal at fixed temperature (77 K) as a function of the applied gate voltage to capacitance-voltage spectroscopy measurements at the same temperature. Moreover, we present results for the temperature dependence of the FWHM for a set of gate voltages. In Sec. IV we develop a model to explain all experimental observations and discuss our observations in Sec. V. We conclude our findings in Sec. VI.

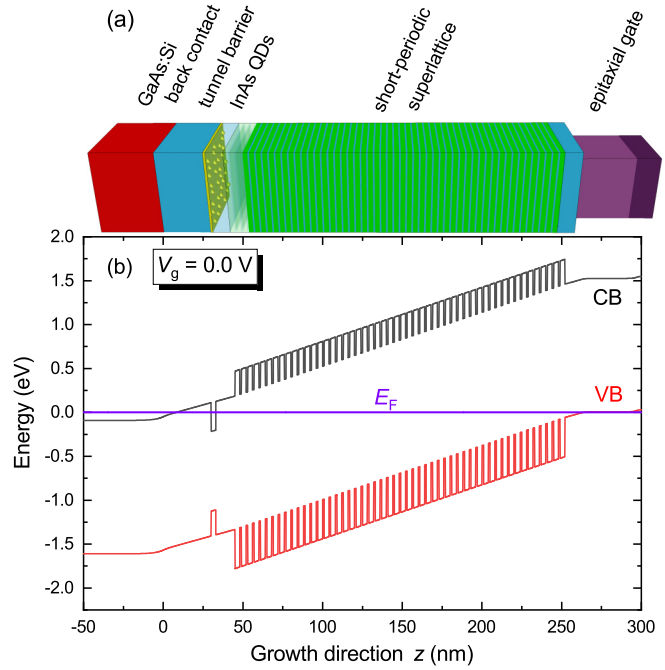

FIG. 1. (a) Schematic layer structure and (b) band structure of the sample at $V_g = 0.0$ V in the conduction (CB) and valence band (VB). The band structure was calculated using a one-dimensional (1D) Poisson-Schrödinger solver [25,26]. The QD layer is shown as a quantum well. The Fermi energy E_F is set as zero of the energy scale and the interface between back contact and tunnel barrier defines the zero of the growth direction axis.

II. EXPERIMENT

The sample consists of InAs self-assembled QDs embedded in an *n-i-p* diode structure (see Fig. 1). It was grown by molecular-beam epitaxy on a (100)-oriented GaAs substrate. A 30-nm GaAs barrier layer (first 5 nm at 575 °C, then 25 nm at 600 °C) separates the QDs from a degenerately *n*-doped GaAs back contact layer, which provides an electron reservoir. The QDs are grown by deposition of approximately 1.9 monolayers InAs at 525 °C over a duration of 54 s yielding a QD density of approximately 10^9 cm^{-2}. QDs grown under similar conditions have radii of (16 ± 2) nm and height of (9 ± 2) nm as evaluated by atomic force microscopy (AFM) measurements. On top of the QDs an 11 nm GaAs capping layer (grown at 500 °C) is deposited. Following the capping layer, a short-periodic superlattice (SPS) consisting of 52 iterations of alternating 3-nm AlAs and 1-nm GaAs layers was grown at 600 °C followed by another 10-nm layer of GaAs. The short-periodic superlattice serves as a current blocking layer between the gate and back contact. The final gate layer is defined by a 35-nm *p*-doped GaAs layer (acceptor density $N_A \approx 2 \times 10^{18}$ cm^{-3}) and a 15-nm highly *p*-doped GaAs layer ($N_A \approx 10^{19}$ cm^{-3}), each using carbon as doping material. For the whole structure, deposition rates of GaAs and AlAs are 0.2 and 0.1 nm/s, respectively. The tunnel barrier, QD capping layer, SPS, and the GaAs layer on top of the SPS are grown without intentional doping and have a background impurity density in the order of 10^{14} cm^{-3}. Gates were defined by mesa etching and contacted by wire bonding.

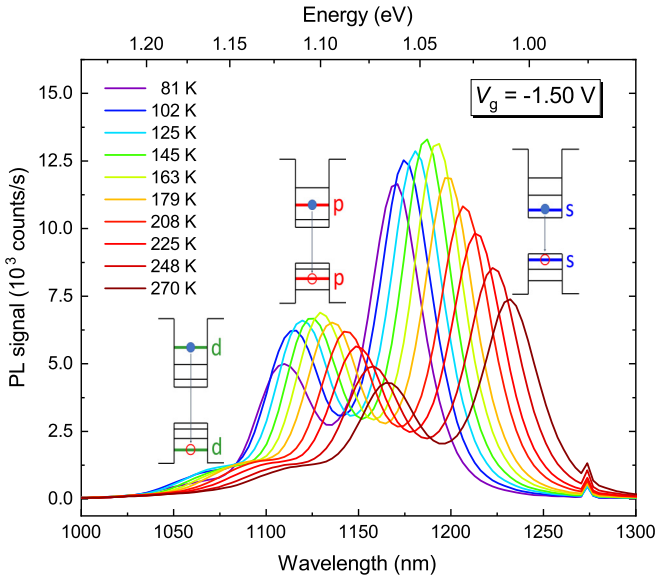

FIG. 2. QD signal in PL spectra at varying temperatures for a gate voltage of $V_g = -1.50$ V. The PL emission initially increases with rising temperature up to 145 or 163 K for the s or p peak, respectively. The small peak at 1276 nm corresponds to the second-order diffraction signal of the laser beam (638 nm) in the spectrometer, which can be neglected for all further considerations. Insets show schematically the QD energy levels and the transitions governing each peak.

Electrical contact to the n-doped back contact was made by indium soldering.

PL measurements are conducted in a variable temperature liquid-nitrogen cryostat (77–300 K) with optical excitation provided by a 638-nm laser diode at a power of 3 mW. The laser beam is focused onto the sample reaching a relatively high intensity (approximately 240 W/cm^2). The PL signal was detected using a near-infrared spectrometer (Ocean Optics NIRQuest512) with a 512-element Hamamatsu InGaAs-array detector. During the temperature-dependent measurement, a gate voltage V_g in a range between -2.50 and $+0.50$ V was applied to the gate and the back contact was connected to the ground.

III. RESULTS

Figure 2 shows an example of PL spectra at a fixed gate voltage of $V_g = -1.50$ V recorded at a set of different temperatures. In PL measurements electron-hole pairs created in the GaAs matrix are captured to QDs and successively fill the s, p, d, and f shells in the QD electronic structure. Recombination of electron-hole pairs occurs mainly between electrons and heavy holes with the same angular momentum quantum number due to optical selection rules. Light-hole transitions are neglected because the lowest-lying few hole states in InAs and $In_{1-x}Ga_xAs$ QDs are known to be dominated by heavy-hole states [27,28]. The spectrum in Fig. 2 was measured at high excitation intensity leading to the s, p, and d peak being visible.

In contrast to the general decrease of the PL signal with rising temperature, an anomalous increase of s-, p-, and d-peak height over a certain temperature range is observed. Note that the d peak is convoluted with a peak at even shorter wavelengths originating from transitions between f levels and is also convoluted with the p peak. To study the deviation from the common Arrhenius behavior further, the wavelength-integrated peak signal of the s, p, and d peaks were evaluated by Gaussian fits to the spectra. Figure 3 shows the Arrhenius plots of the individual wavelength-integrated peak signal for six exemplary gate voltages. For the p and d peak no data are shown for temperatures higher than 260 K because strong convolution of both peaks makes an unambiguous Gaussian fit to the peaks impossible. For all evaluations, the contribution of the wetting layer emission (not shown) is neglected: The wetting layer emission peak shifts from 870 nm at 77 K to 930 nm at 300 K and is thus not relevant for the evaluation of the QD emission.

As seen in Fig. 3, the integrated PL signal of the s peak decreases monotonously with rising temperatures for gate voltages equal to or higher than -0.50 V. At elevated temperatures, the measurement data exhibit a kink (particularly visible at $V_g = -0.50$ V and $T \approx 250$ K), which is a clear sign that two nonradiative recombination channels with different activation energies dominate the quenching of the PL signal. Hence, we use the common Arrhenius model (1) to fit the experimental data assuming two nonradiative recombination channels with activation energies $E_{a,1}$ and $E_{a,2}$ for the s peak. We find that, in this gate voltage range, $E_{a,1} = 33$ meV is approximately constant, whereas $E_{a,2}$ decreases towards more negative gate voltages. We attribute the two nonradiative recombination channels to recombination via hole-related Shockley-Read-Hall recombination ($E_{a,1}$) and thermal escape of electrons and holes from the QDs ($E_{a,2}$) as discussed in more detail in Sec. V.

The plots for more negative gate voltages ($V_g < -0.50$ V) show a conspicuous initial increase in s-peak PL signal for increasing temperature, which is particularly prominent at $V_g = -1.50$ V and cannot be described by the Arrhenius model. The maximum of the integrated PL signal as a function of temperature shifts strongly to higher temperatures from -0.75 to -1.50 V, whereas no significant shift is observed from -1.50 to -2.50 V. The s-peak data for $V_g \leqslant -0.75$ V was fitted using a modified Arrhenius model (4), which is derived below, assuming electrons are provided to the QDs by tunneling from the back contact. For these fits, the activation energy of one nonradiative recombination channel was fixed to $E_{a,1} = 33$ meV, which is the average value obtained from the Arrhenius fits of the s-peak data for $V_g \geqslant -0.50$ V. As this activation energy was found to be independent of the applied gate voltage for $V_g \geqslant -0.50$ V, we assume that it remains independent also at more negative gate voltages, which is a reasonable assumption for Shockley-Read-Hall recombination. On the other hand, $E_{a,2}$ was kept as a free fit parameter.

Similar to the anomalous behavior of the s peak, the p- and especially the d-peak signal also strongly deviate from the Arrhenius model: The p-peak signal increases for rising temperature over a vast temperature range up to higher temperatures for more negative applied gate voltages and then starts to decrease rapidly after reaching a maximum. The common Arrhenius model was used to fit the p-peak data for

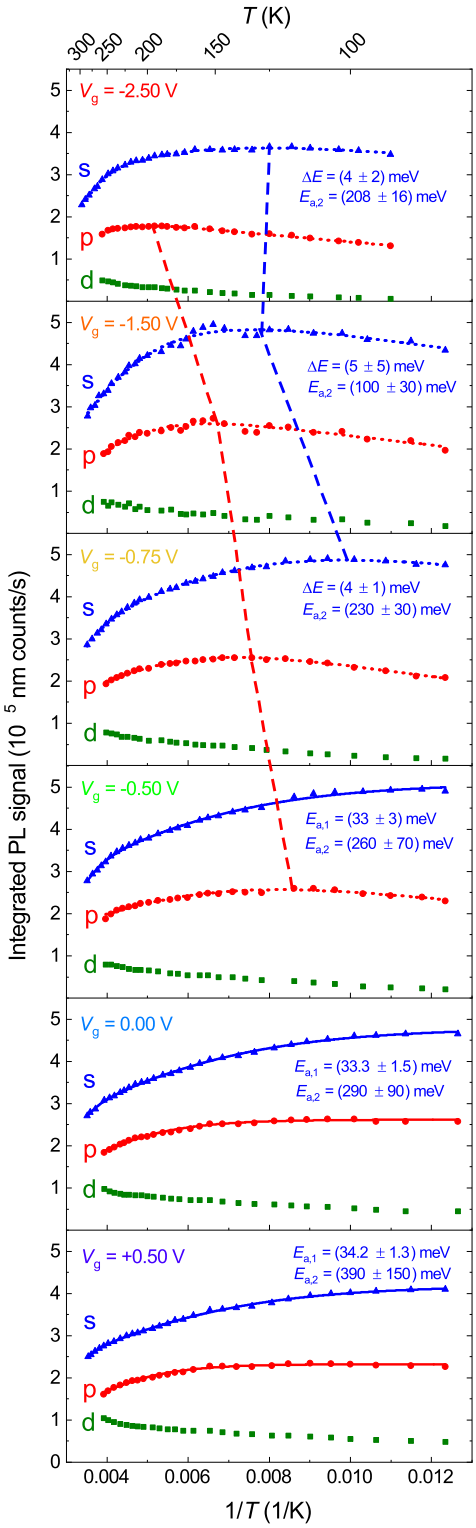

	s-peak	p-peak
I_0 (10^5 nm counts/s)	0 ± 2	0 ± 2
I_1 (10^5 nm counts/s)	95 ± 3	5 ± 3
ΔE (meV)	4 ± 2	7 ± 6
$E_{a,1}$ (meV)	33	120 ± 20
$E_{a,2}$ (meV)	208 ± 16	0
c_1	1.6 ± 0.2	60 ± 50
c_2	$(1.7 \pm 1.1) \cdot 10^3$	0
R^2	0.9973	0.9827
I_0 (10^5 nm counts/s)	0 ± 6	0 ± 8
I_1 (10^5 nm counts/s)	13 ± 12	7 ± 15
ΔE (meV)	5 ± 5	6 ± 18
$E_{a,1}$ (meV)	33	80 ± 20
$E_{a,2}$ (meV)	100 ± 30	0
c_1	1.3 ± 1.4	20 ± 20
c_2	40 ± 40	0
R^2	0.9849	0.8985
I_0 (10^5 nm counts/s)	0 ± 2	0 ± 3
I_1 (10^5 nm counts/s)	13 ± 3	8 ± 6
ΔE (meV)	4 ± 1	7 ± 9
$E_{a,1}$ (meV)	33	50 ± 6
$E_{a,2}$ (meV)	230 ± 30	0
c_1	3.3 ± 0.2	7.1 ± 0.8
c_2	$(4 \pm 5) \cdot 10^3$	0
R^2	0.9984	0.9866
I_0 (10^5 nm counts/s)	5.10 ± 0.05	0.00 ± 0.02
I_1 (10^5 nm counts/s)	0	8 ± 1
ΔE (meV)	0	6 ± 2
$E_{a,1}$ (meV)	33 ± 3	39 ± 7
$E_{a,2}$ (meV)	260 ± 70	0
c_1	2.3 ± 0.3	4.0 ± 0.5
c_2	$(1 \pm 3) \cdot 10^4$	0
R^2	0.9969	0.9630
I_0 (10^5 nm counts/s)	4.79 ± 0.03	2.62 ± 0.01
I_1 (10^5 nm counts/s)	0	0
ΔE (meV)	0	0
$E_{a,1}$ (meV)	33 ± 2	69 ± 4
$E_{a,2}$ (meV)	290 ± 90	0
c_1	2.4 ± 0.2	9 ± 2
c_2	$(2 \pm 6) \cdot 10^4$	0
R^2	0.9986	0.9889
I_0 (10^5 nm counts/s)	4.19 ± 0.02	2.32 ± 0.02
I_1 (10^5 nm counts/s)	0	0
ΔE (meV)	0	0
$E_{a,1}$ (meV)	34 ± 1	78 ± 5
$E_{a,2}$ (meV)	390 ± 150	0
c_1	2.4 ± 0.1	14 ± 3
c_2	$(1 \pm 6) \cdot 10^6$	0
R^2	0.9987	0.9868

FIG. 3. Temperature-dependent wavelength-integrated PL signal of *s*, *p*, and *d* peaks at varying gate voltages V_g. Solid lines are fits using the common Arrhenius model (1), assuming two (one) nonradiative recombination channels for the *s* peak (*p* peak) with activation energies $E_{a,i}$. Dotted lines are fits using the modified Arrhenius model (4) where ΔE is the energy level in the back contact, from which tunneling into the QDs occurs, measured from the Fermi energy. For these fits for the *s*-peak data one of the activation energies was set to the average value $E_{a,1} = 33$ meV obtained from the Arrhenius fits for $V_g \geqslant -0.50$ V while the other is kept variable. For the *p* peaks again only one nonradiative recombination channel with variable activation energy was assumed. Dashed lines across the plots guide the eye along the shift of the maximum position of integrated PL signal. Detailed fit parameters and the coefficient of determination R^2 are given in the adjacent table.

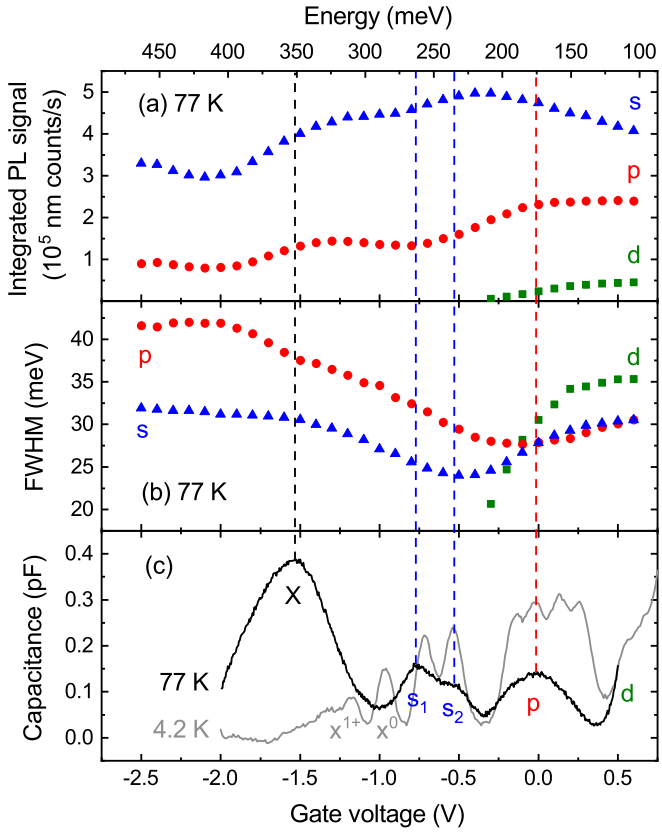

FIG. 4. Integrated PL signal (a) and FWHM (b) of s, p, and d peak at fixed temperature of 77 K in dependence of the gate voltage. (c) $C(V)$ spectrum of the sample measured at 77 K (black) and 4.2 K (grey) under illumination with a 920-nm LED. A background accounting for the diode capacity was subtracted from the measurement data. Vertical lines indicate the positions of the respective $C(V)$ charging peaks at 77 K. For the top axis, the gate voltage was converted to the energy shift at the position of the QDs using a simple lever arm law [29]. The energy at $V_{\mathrm{bi}} = +1.5$ V, which corresponds to the built-in voltage of the n-i-p diode structure, was set as zero of the energy scale.

$V_{\mathrm{g}} \geqslant 0.00$ V and the modified Arrhenius model was used for more negative gate voltages (see Fig. 3). While both models provide excellent agreement with the experimental data, the p-peak PL signal is influenced by additional effects compared to the s peak such as shell filling and thermal redistribution to p levels, which is discussed in more detail below. Note that in contrast to the s-peak data, only one nonradiative recombination channel is used for the fit to the p-peak data, which for $V_{\mathrm{g}} = +0.50$ V has an activation energy $E_{\mathrm{a},1} = 78$ meV in between those identified for the s peak at the same gate voltage. This single recombination channel of the p peaks is mainly attributed to thermal escape as discussed in Sec. V. Fit parameters for all fits are given in the table adjacent to Fig. 3.

The integrated d-peak PL signal increases for all gate voltages over the entire temperature range with a very similar temperature dependence for all gate voltages. However, the absolute value of the d-peak signal is higher for more positive applied gate voltages.

In Fig. 4, we study the connection between the anomalous increase of integrated PL signal to charging of QD levels by electron tunneling from the back contact in more detail at a low temperature of 77 K: The integrated PL signal and the FWHM of the s, p, and d peak as a function of the gate voltage are shown in Figs. 4(a) and 4(b). Note that in contrast to the temperature-dependent measurements, the spectra were measured with a SPEX 500M monochromator using the same excitation laser and power. The scale of the monochromator measurement was converted to the scale of the spectrometer measurement to allow for comparison of the data. After a slight decrease of the integrated PL signal from -2.5 to -2.1 V for both the s and p peak, the PL signal increases with a plateau-shaped feature around -1.2 V. The s-peak signal reaches a maximum at $V_{\mathrm{g}} = -0.3$ V and starts to decrease for higher voltages. The p-peak signal reaches another plateau from -0.2 to $+0.6$ V. A d peak becomes visible in the spectrum for gate voltages higher than -0.3 V and the integrated PL signal of the d peak increases towards higher gate voltages. The FWHM of the s and p peak in Fig. 4(b) decreases for increasing gate voltage reaching a minimum at $V_{\mathrm{g}} = -0.5$ V and $V_{\mathrm{g}} = -0.1$ V, respectively. For the d peak the FWHM increases monotonously towards higher gate voltages.

The findings from these PL measurements are complemented by the characterization of the QD diode sample via capacitance-voltage [$C(V)$] spectroscopy. In $C(V)$ spectroscopy the capacitive tunneling current between the back contact and the QDs with a small ac voltage $V_{\mathrm{ac}} = 10$ mV applied to the gate is measured as a function of dc gate voltage superimposed to the ac voltage. When the Fermi level in the back contact is in resonance with an energy level in the QDs, electrons can tunnel in and out of the QDs, creating a tunneling current, which is measured as a capacitance change.

Figure 4(c) shows the $C(V)$ spectrum of the investigated sample at 77 and 4.2 K measured under illumination by a 920-nm LED. The peak features correspond to different charge-carrier filling levels of the QDs, where, e.g., s_1 corresponds to charging of the first electron to a previously empty QD and s_2 to charging of the second electron. Coulomb repulsion lifts the spin degeneracy of the QD energy levels. Additionally, $C(V)$ spectra under illumination show peaks at lower gate voltages than the s peaks, which correspond to the charging of exciton states X consisting of one s-state electron and one (X^0) or two holes (X^{1+}) in the QDs [10,30,31]. At 77 K, the different states can only be distinguished for the s states, which show a peak at $V_{\mathrm{g}} = -0.75$ V (s_1) and a shoulder at approximately $V_{\mathrm{g}} = -0.6$ V (s_2). The excitonic and p states show broad peaks, which each comprise multiple charge states. At 4.2 K, two distinct excitonic as well as four p peaks are visible. While the s-, p-, and d-peak positions only shift slightly from 4.2 to 77 K, exciton peaks are shifted strongly towards negative gate voltages [31]. The top axis of Fig. 4 shows the shift of the energy levels in the QDs E_{QD}, which applies to both PL as well as $C(V)$ spectroscopy measurements. E_{QD} is determined directly from the gate voltage using a conventional lever arm approach [29]:

$$E_{\mathrm{QD}} = \frac{e}{\lambda}(V_{\mathrm{bi}} - V_{\mathrm{g}}), \tag{2}$$

where e is the elementary charge and $V_{\mathrm{bi}} = +1.5$ V is the built-in voltage of the n-i-p diode structure. The lever arm

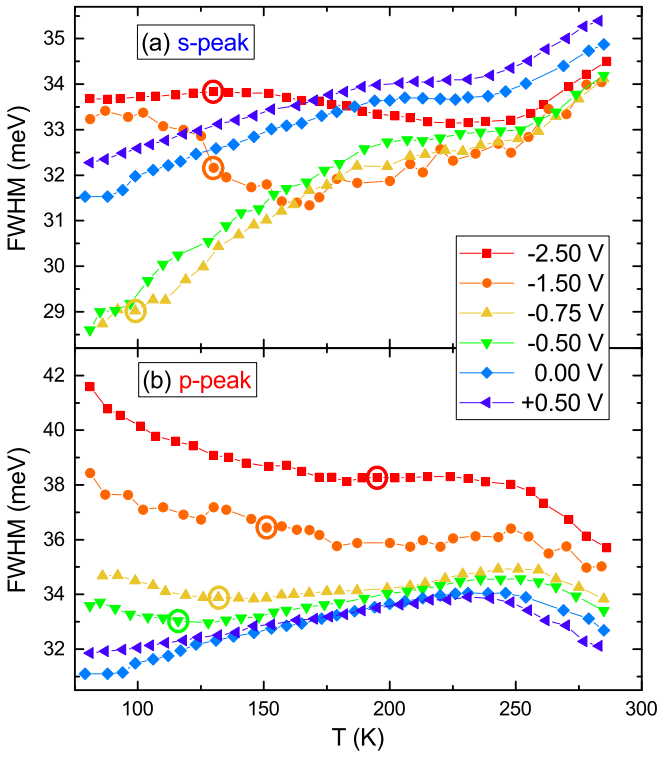

FIG. 5. FWHM of the *s* and *p* peak as a function of temperature at different gate voltages. Open circles indicate the temperature at which the maximum integrated PL signal of the respective peak is observed in Fig. 3. Solid lines are a guide to the eye.

factor $\lambda = d_{\text{total}}/d_{\text{QD}}$ is determined from the sample structure. The distance from the end of the back contact to the start of the epitaxial gate layer or the QD layer is denoted as $d_{\text{total}} = 259$ nm and $d_{\text{QD}} = 30$ nm, respectively. In (2), the energy-level position at the built-in voltage V_{bi} was set as zero of the energy scale.

By comparing the $C(V)$ spectrum at 77 K to the voltage dependent PL signal at the same temperature in Fig. 4(a), one can see that the range in which the PL signal of a peak is high roughly corresponds to the gate voltage region in which the corresponding states are charged in the $C(V)$ measurement. Since in the exciton peaks electrons tunnel into *s* states, the exciton peaks are also compared to the *s*-peak PL signal. Furthermore, the minimum of the FWHM of the *s* and *p* peak is also located in this gate voltage range.

Figure 5 shows the FWHM of the *s*, *p*, and *d* peak depending on temperature at varying applied gate voltages. As seen before in Fig. 4(b) for the *s* and *p* peak at low temperatures below 100 K the FWHM is observed to be lowest in the gate voltage ranges between -0.75 and -0.50 V for the *s* peak and at 0.00 V for the *p* peak. As a function of temperature the *s* peak shows a minimum in the FWHM for $V_g \leqslant -1.50$ V only, otherwise the FWHM increases monotonously with temperature with a plateau between 200 and 250 K. Open circles in Fig. 5 indicate the temperature at which the maximum integrated PL signal is measured for the respective gate voltage in Fig. 3. For the *s* peak, no significant correlation between this temperature and the minimum of the FWHM is observed. The *p*-peak FWHM increases monotonously with rising temperature up to 250 K for positive gate voltages. For negative gate voltages, the FWHM decreases until a minimum is reached and then starts to increase again up to approximately 250 K. The position of the local minimum of the *p*-peak FWHM shifts to higher temperatures and roughly corresponds to the position of the maximum integrated PL signal in Fig. 3. For higher temperatures than 250 K, the FWHM decreases for all applied gate voltages. For the *d* peak no data are shown because the convolution between the *d* and *f* peak in the spectrum at high temperatures does not allow for a precise evaluation of the FWHM.

IV. MODEL

We first consider features reported in previous studies and then develop a model explaining our findings. An anomalous increase of the integrated PL signal has been explained by carriers trapped in shallow localization sites (shallow QDs) in the potential landscape at low temperatures [18,24]. Increasing the temperature causes the trapped carriers to be detrapped and then recaptured to deeper localization sites (deeper QDs). Since the quantum confinement is stronger in deep localization sites, the radiative recombination rate is assumed to be higher for carriers there, explaining the initial increase of the PL signal with rising temperature. The thermal redistribution effect to deeper QDs in these studies was reported to also lead to a minimum of the FWHM of the PL peak at the same temperature, at which the maximum PL signal is measured. Similarly, an anomalous temperature dependence has also been explained by thermally activated redistribution between directly coupled QDs in close proximity [17]. Direct coupling of QDs can be assumed to be negligible in our measurements as the QD density in our samples is approximately 10^9 cm^{-2} and thus two orders of magnitude lower than reported in the study assuming direct coupling. The thermally activated carrier redistribution into deeper QDs may still play a role in our samples, however, this effect does not explain the voltage dependence of the integrated PL signal observed in Figs. 3 and 4.

Popescu *et al.* investigated InAs QDs in a strained $Ga_{0.85}In_{0.15}As$ quantum well and observed an anomalous increase of PL signal with rising temperature arising from a strain field induced potential barrier at the interface between QDs and the quantum well [23]. Such a barrier inhibits charge-carrier capture to the QDs at low temperatures. At elevated temperatures, charge carriers can overcome the barrier due to thermal excitation and are thus more effectively captured into QDs. However, this mechanism does not suffice to explain the gate voltage dependence observed in our study: If this mechanism caused the anomalous increase of PL signal in our measurements, we would expect a particularly strong anomaly in the case of an almost flat band structure, i.e., at positive gate voltages. For more negative gate voltages the band structure is strongly tilted upwards, which diminishes the effect of an interface potential barrier as small as 7.3 meV as reported in [23]. These predictions are contrary to our measurements, which show a particularly strong anomaly at negative gate voltages and no anomaly at positive voltages.

Our findings for the temperature dependence of the integrated PL signal in Fig. 3 show a strong gate voltage

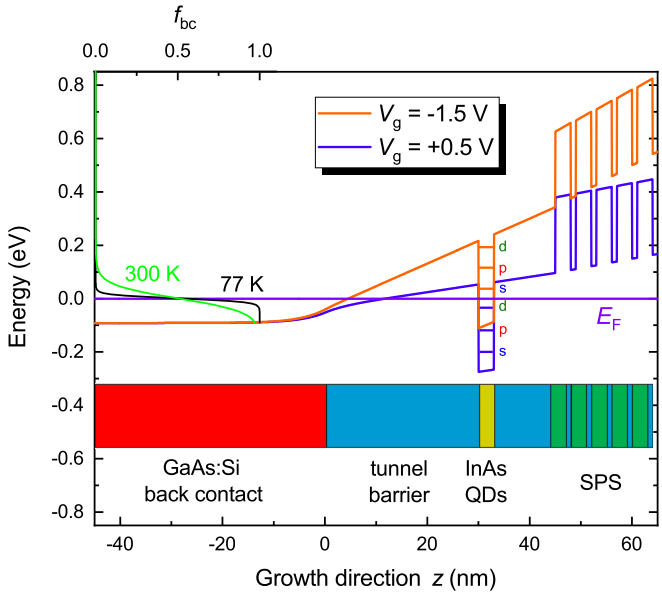

FIG. 6. Conduction-band structure of the sample in the QD region at $V_g = +0.5$ V and $V_g = -1.5$ V. The band structure was calculated using a 1D Poisson-Schrödinger solver [25,26]. The QD layer is shown as a quantum well and approximate *s*-, *p*-, and *d*-energy levels in the QDs are indicated. The Fermi energy E_F is set as zero of the energy scale and the interface between back contact and tunnel barrier defines the zero of the growth direction axis. The electron Fermi distribution in the back contact f_{bc} is shown at 77 and 300 K (top axis).

dependence and the comparison of the integrated PL signal with the charging of the respective QD energy states in the $C(V)$ spectra (Fig. 4) shows a direct correlation between peak signal and gate voltage. Hence, we conclude that excessive electron tunneling between the back contact and the QDs as well as loss of intensity due to Auger effects for highly charged states play a major role here. Under these assumptions we derived the following model to explain the observations: At negative gate voltages, the external field causes electrons from electron-hole pairs generated by illumination in the GaAs matrix or the wetting layer to move into the back contact. In contrast, holes cannot move to the gate as effectively, mainly due to the presence of the short-periodic superlattice, providing a high barrier in the valence band. Therefore, at negative gate voltages on average there are more holes than electrons stored in the QDs and not all generated electron-hole pairs can recombine. Thus, electrons are the minority charge carriers in this case. As a consequence, an increase of PL signal can be caused by additional electrons tunneling into the QD levels from the back contact and then recombining with holes trapped inside the QDs. This happens as soon as electrons find accessible levels in the QDs due to more positive gate bias or thermal activation. The levels usually found in $C(V)$ spectroscopy are lowered here due to Coulomb attraction of the stored holes, the exciton binding energy. At higher temperatures, the Fermi distribution function in the back contact smears out, i.e., more electrons are available at higher energies, which can tunnel into the QD levels (see Fig. 6), resulting in the anomalous increase of the PL signal with rising temperatures observed in Fig. 3. At very high temperatures, nonradiative recombinations via defect centers and thermal escape from the QDs start to dominate, causing the usual quenching of the PL.

For the *s*-peak transition, the electron tunnel coupling between QDs and back contact can be accounted for in a phenomenological way by modifying the Arrhenius model: The rate equation for the exciton population n corresponding to the *s*-peak transition is given by

$$\frac{\partial n}{\partial t} = \gamma_e - n\gamma_r - n\sum_i \gamma_{nr,i} + \gamma_t f_{bc}(\Delta E, T), \qquad (3)$$

where γ_e is the laser induced generation rate of excitons in the QDs, γ_r is the radiative and $\gamma_{nr,i}$ the nonradiative recombination rate, and the sum over i is taken over all possible nonradiative recombination channels. Note that in the experiment, excitation is performed above the band gap of GaAs. Therefore, most charge carriers that generate the QD PL signal need to be captured to the QDs before recombination. The rate γ_e comprises the free charge-carrier generation rate as well as the capture rate into the QDs. The last term in (3) is added compared to the derivation of the usual Arrhenius model to account for electron tunneling, which is proportional with a rate constant γ_t to the Fermi distribution function in the back contact $f_{bc}(\Delta E, T) = 1/[1 + \exp(\frac{\Delta E}{k_B T})]$. Here ΔE is the energy level in the back contact, from which electrons tunnel into the QDs, measured with respect to the Fermi energy. Adding this term to the rate equation is a valid approximation only if electrons are minority charge carriers in the QDs, i.e., at negative gate voltages. Nonradiative recombination channels are commonly assumed to be thermally activated with an activation energy $E_{a,i}$ according to $\gamma_{nr,i} = \gamma_{0,i}\exp(-\frac{E_{a,i}}{k_B T})$ [22]. Solving (3) for the steady state ($\partial n/\partial t = 0$) and assuming that the PL signal I is proportional to $n\gamma_r$ one obtains

$$I = \frac{I_0 + I_1 f_{bc}(\Delta E, T)}{1 + \sum_i c_i \exp\left(-\frac{E_{a,i}}{k_B T}\right)} \qquad (4)$$

with $c_i = \gamma_{0,i}/\gamma_r$ and parameters I_0 and I_1, which are proportional to γ_e and γ_t, respectively. For $I_1 = 0$ (no tunnel coupling to the back contact) this model reduces to (1).

V. DISCUSSION

In this section, we discuss the results and model presented in Secs. III and IV. We start by interpreting the observations of anomalous PL temperature dependence of the *s* peak in the framework of our model in different gate voltage regions and discuss the role of the two nonradiative recombination channels found in the experiment. In this context, we argue that the tunnel coupling between QDs and electron reservoir leads to increased PL emission in those gate voltage regions in which the respective QD states are charged in the $C(V)$ measurements. Following this discussion, we elaborate on the increased complexity of emission from *p* and *d* states: We show that our model still describes the experimental data, however, the fit parameters become effective parameters comprising contributions from different mechanisms. Last, we

discuss the influence of tunnel coupling on the FWHM of the QD emission peaks.

Using the usual Arrhenius model (1) and the modified model (4), we can now discuss the *s*-peak temperature dependence observed in Fig. 3. For gate voltages equal to or larger than −0.50 V, the *s*-peak data is well approximated by the usual Arrhenius model with two nonradiative recombination channels ($i = 1, 2$). In this voltage range, there is always at least one QD energy level located below the Fermi energy. As a consequence, electrons are sufficiently supplied to the QDs and thus tunnel coupling to the back contact does not have a strong impact on the temperature dependence of the PL signal. As discussed initially, it is reasonable to assume that at positive gate voltages hole-related defect states dominate the quenching of the PL signal. If this theory holds true, the channel with low activation energy $E_{a,1} = 33$ meV can be mostly attributed to Shockley-Read-Hall recombination via such states. As one would expect for Shockley-Read-Hall recombination, the activation energy of this channel is approximately constant as a function of V_g: The energy level of the defect states barely changes with respect to the QD energy levels when the gate voltage is changed.

The second channel with significantly higher activation energy $E_{a,2}$, which tends to lower values towards more negative gate voltages, is likely related to thermal escape from the QDs: The activation energy of this channel at $V_g = 0.00$ V is $E_{a,2} = 290 \pm 90$ meV. This value roughly corresponds to the band offset between the electron ground state in the QDs and the wetting layer states in the conduction band, which is commonly between 230 and 270 meV [31,32]. Electrons may also escape from QDs by being redistributed to higher levels and then tunneling out through the tunnel barrier. Therefore, the reduced tunnel barrier at more negative gate bias effectively leads to a decrease of the associated activation energy as shown in Fig. 3.

Thermal redistribution from *s* to higher levels additionally decreases the PL signal, however, the activation energy for this process is on the order of the electron energy level spacing (approximately 45 meV) and thus close to the nonradiative recombination channel $E_{a,1} = 33$ meV. Therefore, thermal redistribution cannot be resolved as a separate quenching mechanism but is rather comprised in the rate of the first nonradiative recombination characterized by $E_{a,1}$. Note that thermal redistribution alone cannot account for the observations of anomalous temperature dependence of the PL signal at gate voltages $V_g \leqslant -0.75$ V as it does not explain the initial increase of the *s*-peak signal.

Assuming the two nonradiative recombination channels and conducting the fitting as described in Sec. III, the modified Arrhenius model describes the anomalous temperature dependence of the *s*-peak integrated PL signal in Fig. 3 well. The fit value of ΔE is determined to be on the order of few meV for all gate voltages with no significant trends. This result indicates that tunneling into the QDs mostly occurs from energy levels in the back contact slightly above the Fermi energy. Note that while only a single tunneling channel is assumed in the model in (4), there may exist multiple channels (e.g., for tunneling into positively charged exciton states containing a different number of holes) making ΔE an effective value accounting for all these channels. Considering the shift of the QD energy levels as a function of the gate voltage, one would expect that ΔE shifts towards higher values for more negative applied gate voltages, however, we do not observe such behavior in the measurements. The reason for this might be that for more negative gate voltages the hole occupation in the QDs increases, causing increased Coulomb attraction for electrons. As a consequence, the energy levels, which electrons from the back contact can tunnel into, are lowered.

Note that for gate voltages lower than or equal to −0.75 V the Fermi energy is shifted below the QD *s* levels and thus the rate for electron tunneling out of the QDs into the back contact severely increases. Therefore, in this gate voltage range the PL signal at low temperatures $T \to 0$ K is expected to be significantly decreased. As a result, the parameter I_0 in the modified Arrhenius fit, which corresponds to the wavelength-integrated PL signal at $T \to 0$ K in the case of no tunnel coupling to the back contact, is determined as $I_0 = 0$ nm counts/s with large errors. The reason for this is the limited temperature range of the measurement towards low temperatures, which does not allow for a more accurate determination of I_0.

The levels in the QDs, that electrons may tunnel into depend on the tilting of the conduction band and thus on the applied gate voltage. The particularly strong initial increase of the integrated PL signal for the *s* peak at $V_g = -1.50$ V is best understood by also taking into consideration the observations made in Fig. 4(a) for the comparison of the integrated PL signal to the $C(V)$ spectrum at 77 K. In the gate voltage range around −1.5 V an increased PL signal of the *s* peak is observed resulting in a plateau-shaped feature, which can be explained by electrons being able to tunnel into positively charged exciton states. The enhanced luminescence of the *p* peak in the same gate voltage range is presumably caused by thermal redistribution from *s* into *p* states and shell filling due to the presence of more electrons in the QDs. The strong tunnel coupling to exciton states for $V_g = -1.50$ V causes the integrated PL signal in Fig. 3 to increase up to higher temperatures than for $V_g = -0.75$ V. For highly negative gate voltages ($V_g = -2.50$ V), the hybridization of QD hole states in the valence band with extended states in the wetting layer or the GaAs matrix [33] can effectively cause shielding of the external electric field, explaining why no further shift of the maximum position of integrated PL signal is observed from −1.50 to −2.50 V.

The integrated *s*-peak PL signal in Fig. 4(a) is further increased for gate voltages between −0.7 and −0.2 V. This approximately corresponds to the gate voltage range, in which *s* states are charged in $C(V)$ spectroscopy at 77 K [Fig. 4(c)]. However, in this gate voltage range barely any anomalous temperature dependence of the integrated PL signal is observed in Fig. 3 as QDs are already sufficiently occupied with electrons. Hence, tunnel coupling does not affect the temperature dependence of the PL emission. Similar to the observations for the *s* peak, the *p*-peak PL signal in Fig. 4 is also increased for gate voltages higher than −0.2 V corresponding to the gate voltage range, in which the *p* states are charged in $C(V)$ spectroscopy. The behavior of the *d* peak is explained in the same way. Overall, these observations are evidence that the thermally enhanced tunnel coupling mechanism is particularly important at low temperatures in the gate voltage

ranges in which the respective energy levels in the QDs are charged in $C(V)$ measurements but will only cause anomalous temperature dependence of the PL emission if electrons in the QDs are minority charge carriers in the respective states.

For gate voltages higher than -0.3 V in Fig. 4(a), the s-peak luminescence decreases as the s states and positively charged excitonic states in the QDs are shifted below the conduction-band edge of the back contact and thus no direct tunneling processes into these states can occur anymore. Moreover, Auger recombinations for negatively charged excitons further decrease the PL signal. The overall decrease of the PL signal of all peaks towards lower gate voltages in Fig. 4 is on the one hand explained by the lower electron occupation as well as the increased influence of Auger recombinations of multiple hole states. On the other hand, the quantum confined Stark effect may decrease the radiative recombination rate [34].

The initial decrease of s- and p-peak integrated PL signal from -2.5 to -2.1 V in Fig. 4(a) cannot be explained by electron tunneling into QD states. At such high negative voltages, hybridization of hole states in the QDs and in the wetting layer may occur [33] and feed charges to the QDs efficiently.

Accurately describing the temperature dependence of the p and d peaks in Fig. 3 is more complicated than for the s peak due to additional temperature-dependent effects, particularly the influence of thermal redistribution to and from these levels as well as shell filling depending on the occupation of s states. The multitude of possible effects significantly increases the complexity of the rate equations describing the state occupation. However, in a more complex fitting model the determination of all parameters becomes increasingly difficult. This problem already arises for the determination of the fit parameters for the s-peak fits in Fig. 3, which in some instances possess large errors as discussed above for the parameter I_0.

Despite the complexity of the problem, the fit using the modified Arrhenius model (4) provides excellent agreement with the experimental data also for the p peak. Only one nonradiative recombination channel with activation energy $E_{a,1}$ was used to fit the experimental p-peak data in Fig. 3, whereas two channels were used for the s-peak data. The reason for this is that the p-peak temperature dependence of PL emission is much more strongly dominated by thermal escape of electrons or holes from QDs because p states are located at higher energies compared to s states. This significantly reduces the potential barrier for carrier escape. Second, the reduced activation energy of thermal escape implies that the difference in activation energy between thermal escape and Shockley-Read-Hall recombination is decreased for the p-peak compared to the s-peak emission. For these reasons, Shockley-Read-Hall recombination via defect states is not resolved as a separate recombination path, although it should be occurring also for p states. Also note that at highly negative gate voltages the p-peak PL signal is strongly anomalous and increases up to very high temperatures. This behavior is caused in part by the thermally enhanced tunnel coupling to the back contact discussed above. On the other hand, shell filling and thermal redistribution within the QDs also contribute to this behavior for the p peak. As the modified Arrhenius model does not take the latter two effects explicitly into account and the temperature range in the measurement is limited, the determination of the fit parameters ΔE and $E_{a,1}$ is ambiguous in this case and these parameters should be considered as effective parameters containing the influences of all these processes.

Since the complexity of the problem does not allow for a quantitative discussion of the fit parameters for the p as well as the d peak, which cannot be fitted using the modified Arrhenius model, we restrict our discussion to a qualitative description: For higher energy peaks in the spectrum, the anomalous initial increase of PL signal with rising temperature is more pronounced and persists up to higher temperatures compared to the s peak at the same gate voltage (see Fig. 3). The reason for this is that higher energy levels in the QDs are generally less populated than lower energy levels because the relaxation time from high to low energy levels within the QDs is on the order of 50 ps [35] and thus significantly lower than the recombination time of electron-hole pairs, which is approximately 1 ns [36]. The lower occupation of higher energy states leads to higher energy peaks being influenced more significantly by electron tunneling from the back contact. The presence of thermal redistribution and shell filling effects further causes the p and d peaks to increase in integrated PL signal up to higher temperatures at negative gate voltages. For $V_g \geqslant 0.00$ V, these effects still cause a steeper shape of the measurement curve of the integrated PL signal in Fig. 3.

At 77 K, a minimum in the FWHM as a function of gate voltage is observed for the s and p peak in the gate voltage ranges, in which the s or p states are charged in $C(V)$ spectroscopy as seen in Fig. 4(b) as well as in the low-temperature regime in Figs. 5(a) and 5(b). At these voltages, the enhanced recombination of charge carriers in the QDs leads to a lower number of possible charge states. As highly charged exciton states at negative gate voltages enable a multitude of different transitions, the decreased number of charge states leads to a lower FWHM of the emission peaks in the gate voltage ranges where tunnel coupling to the back contact is strong. For voltages more positive than the peak charging voltage, the FWHM increases due to the higher electron state filling in the QDs and hybridization of QD energy levels with levels in the wetting layer in the conduction band [33]. In contrast to the observations for the s and p peaks, the d-peak FWHM in Fig. 4(b) increases monotonously for increasing gate voltage despite the d peaks being charged around $V_g = +0.5$ V. At such positive voltages, the QDs are already filled with a high number of electrons. Due to Coulomb repulsion, this causes the d states to be shifted upwards resulting in increased wetting layer hybridization with the d states.

The minimum in the FWHM as a function of temperature observed for the s peak at $V_g \leqslant -1.50$ V and for the p peak at all negative gate voltages [see Figs. 5(a) and 5(b)] is also explained by the increasing influence of tunnel coupling to the back contact with rising temperature decreasing the FWHM. Note that in this case tunneling into s states also decreases the FWHM of the p peak as the total number of charge carriers on the QDs is annihilation. Superimposed to these effects is the increased carrier-phonon interaction at higher temperatures leading to an increase of the FWHM [37]. Additionally, at high temperatures, thermal redistribution of carriers in the

QDs may also increase the number of initial and final states for electron-hole recombination and thus broaden the emission peaks. The superposition of these effects effectively causes the minimum of the FWHM.

For the *s*-peak data in Fig. 5 at $V_g \leqslant -1.50$ V the minimum position of the FWHM is always found at a higher temperature than the maximum position of integrated PL signal. The minimum of the FWHM is observed when the tunnel coupling of electrons from the back contact is so high that the X^0 exciton, which besides singly charged excitons has the lowest number of possible initial and final states for recombination, dominates the PL emission. The X^0 also possesses the highest radiative recombination rate compared to other excitons as it is not affected by Auger recombination. However, the maximum of the integrated PL signal is measured at a lower temperature because the PL signal is superimposed with the decrease of PL emission due to thermally activated nonradiative recombination via defect states and thermal escape from the QDs. Note that for the *p*-peak data, a good correlation between the position of the minimum in the FWHM and the maximum in the integrated PL signal is observed. However, this correlation is ambiguous as the *p*-peak emission is also enhanced by thermal redistribution and shell filling.

At temperatures above 260 K, the *p* and *d* peak are strongly convoluted and thus the Gaussian fit curves interfere making an unambiguous evaluation of the respective FWHMs no longer possible. The strong decrease of *p*-peak FWHM in this temperature range is caused by this interference and is not related to a physical effect.

VI. CONCLUSION

In this study we have demonstrated an anomalous temperature dependence of the ground- and excited-state PL signal from self-assembled InAs QDs embedded in an *n-i-p* diode structure between 77 and 300 K when sufficiently negative gate voltages are applied to the structure. For weakly negative and positive gate voltages, the ground-state emission temperature dependence is well described by an Arrhenius model. In contrast to previous studies on the topic, the anomalous temperature dependence at more negative gate voltages was explained for the ground-state transition by a modified Arrhenius model taking into account electron tunneling from the back contact into the QDs, which depends on the Fermi distribution function in the back contact of the diode structure. This model is further supported by the comparison of PL results to $C(V)$ spectroscopy measurements. Despite the increased complexity of the description for excited-state transitions due to shell filling effects as well as thermal redistribution among the QD levels, our modified Arrhenius model shows excellent agreement with the experimental results. We conclude that the phenomena demonstrated in this paper are of universal importance for temperature-dependent characterization and operation of QD diode structures, in which QDs are coupled to an electron reservoir via a tunneling barrier.

ACKNOWLEDGMENTS

We gratefully acknowledge support from DFG-TRR160, DFG (Grants No. GE2141/5-1 and No. LU2051/1-1), BMBF - Q.Link.X (Grant No. 16KIS0867), and the DFH/UFA CDFA-05-06 as well as IMPRS-SurMat.

A.R.K. performed the experiment and evaluated the data. A.R.K. and A.L. wrote the manuscript and devised the model. All authors contributed in part to the experiment, data acquisition, interpretation and sample growth. A.L. supervised the project.

[1] O. Shchekin and D. Deppe, Appl. Phys. Lett. **80**, 3277 (2002).
[2] Y. Qiu, P. Gogna, S. Forouhar, A. Stintz, and L. Lester, Appl. Phys. Lett. **79**, 3570 (2001).
[3] D. Huffaker, G. Park, Z. Zou, O. Shchekin, and D. Deppe, Appl. Phys. Lett. **73**, 2564 (1998).
[4] D. Bimberg, N. Kirstaedter, N. Ledentsov, Z. I. Alferov, P. Kop'Ev, and V. Ustinov, IEEE J. Sel. Top. Quantum Electron. **3**, 196 (1997).
[5] P. Michler, A. Kiraz, C. Becher, W. Schoenfeld, P. Petroff, L. Zhang, E. Hu, and A. Imamoglu, Science **290**, 2282 (2000).
[6] M. Pelton, C. Santori, J. Vucković, B. Zhang, G. S. Solomon, J. Plant, and Y. Yamamoto, Phys. Rev. Lett. **89**, 233602 (2002).
[7] R. S. Daveau, K. C. Balram, T. Pregnolato, J. Liu, E. H. Lee, J. D. Song, V. Verma, R. Mirin, S. W. Nam, L. Midolo *et al.*, Optica **4**, 178 (2017).
[8] M. Ediger, G. Bester, A. Badolato, P. Petroff, K. Karrai, A. Zunger, and R. Warburton, Nat. Phys. **3**, 774 (2007).
[9] M. Ediger, G. Bester, B. D. Gerardot, A. Badolato, P. M. Petroff, K. Karrai, A. Zunger, and R. J. Warburton, Phys. Rev. Lett. **98**, 036808 (2007).
[10] P. A. Labud, A. Ludwig, A. D. Wieck, G. Bester, and D. Reuter, Phys. Rev. Lett. **112**, 046803 (2014).
[11] A. Kurzmann, A. Ludwig, A. D. Wieck, A. Lorke, and M. Geller, Nano Lett. **16**, 3367 (2016).
[12] A. K. Rai, S. Gordon, A. Ludwig, A. D. Wieck, A. Zrenner, and D. Reuter, Phys. Status Solidi B **253**, 437 (2016).
[13] A. Kurzmann, A. Ludwig, A. D. Wieck, A. Lorke, and M. Geller, Appl. Phys. Lett. **108**, 263108 (2016).
[14] E. C. Le Ru, J. Fack, and R. Murray, Phys. Rev. B **67**, 245318 (2003).
[15] L. Brusaferri, S. Sanguinetti, E. Grilli, M. Guzzi, A. Bignazzi, F. Bogani, L. Carraresi, M. Colocci, A. Bosacchi, P. Frigeri *et al.*, Appl. Phys. Lett. **69**, 3354 (1996).
[16] H. Lee, W. Yang, and P. C. Sercel, Phys. Rev. B **55**, 9757 (1997).
[17] Z. Ma, K. Pierz, and P. Hinze, Appl. Phys. Lett. **79**, 2564 (2001).
[18] A. Polimeni, A. Patanè, M. Henini, L. Eaves, and P. C. Main, Phys. Rev. B **59**, 5064 (1999).
[19] S. Sanguinetti, M. Henini, M. Grassi Alessi, M. Capizzi, P. Frigeri, and S. Franchi, Phys. Rev. B **60**, 8276 (1999).
[20] W. Shockley and W. T. Read, Phys. Rev. **87**, 835 (1952).

[21] C. Rothfuchs, N. Kukharchyk, M. K. Greff, A. D. Wieck, and A. Ludwig, Appl. Phys. B **122**, 49 (2016).
[22] M. Leroux, N. Grandjean, B. Beaumont, G. Nataf, F. Semond, J. Massies, and P. Gibart, J. Appl. Phys. **86**, 3721 (1999).
[23] D. P. Popescu, P. G. Eliseev, A. Stintz, and K. J. Malloy, Semicond. Sci. Technol. **19**, 33 (2003).
[24] G.-E. Weng, W.-R. Zhao, S.-Q. Chen, H. Akiyama, Z.-C. Li, J.-P. Liu, and B.-P. Zhang, Nanoscale Res. Lett. **10**, 31 (2015).
[25] G. L. Snider, 1D Poisson-Schrödinger solver, https://www3.nd.edu/~gsnider/.
[26] I.-H. Tan, G. Snider, L. Chang, and E. Hu, J. Appl. Phys. **68**, 4071 (1990).
[27] G. Bester, S. Nair, and A. Zunger, Phys. Rev. B **67**, 161306(R) (2003).
[28] D. Reuter, P. Kailuweit, A. D. Wieck, U. Zeitler, O. Wibbelhoff, C. Meier, A. Lorke, and J. C. Maan, Phys. Rev. Lett. **94**, 026808 (2005).
[29] H. Drexler, D. Leonard, W. Hansen, J. P. Kotthaus, and P. M. Petroff, Phys. Rev. Lett. **73**, 2252 (1994).
[30] S. R. Valentin, J. Schwinger, P. Eickelmann, P. A. Labud, A. D. Wieck, B. Sothmann, and A. Ludwig, Phys. Rev. B **97**, 045416 (2018).
[31] F. Brinks, A. D. Wieck, and A. Ludwig, New J. Phys. **18**, 123019 (2016).
[32] W. Lei, M. Offer, A. Lorke, C. Notthoff, C. Meier, O. Wibbelhoff, and A. Wieck, Appl. Phys. Lett. **92**, 193111 (2008).
[33] M. C. Löbl, S. Scholz, I. Söllner, J. Ritzmann, T. Denneulin, A. Kovacs, B. E. Kardynał, A. D. Wieck, A. Ludwig, and R. J. Warburton, arXiv:1810.00891v1 [Phys. Rev. X (to be published)].
[34] G. W. Wen, J. Y. Lin, H. X. Jiang, and Z. Chen, Phys. Rev. B **52**, 5913 (1995).
[35] R. Heitz, M. Veit, N. N. Ledentsov, A. Hoffmann, D. Bimberg, V. M. Ustinov, P. S. Kop'ev, and Z. I. Alferov, Phys. Rev. B **56**, 10435 (1997).
[36] B. Ohnesorge, M. Albrecht, J. Oshinowo, A. Forchel, and Y. Arakawa, Phys. Rev. B **54**, 11532 (1996).
[37] M. Bayer and A. Forchel, Phys. Rev. B **65**, 041308(R) (2002).